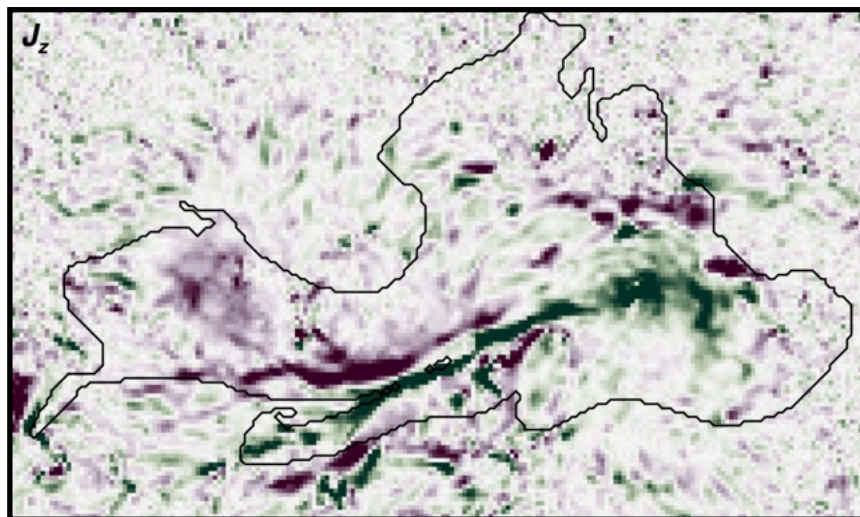
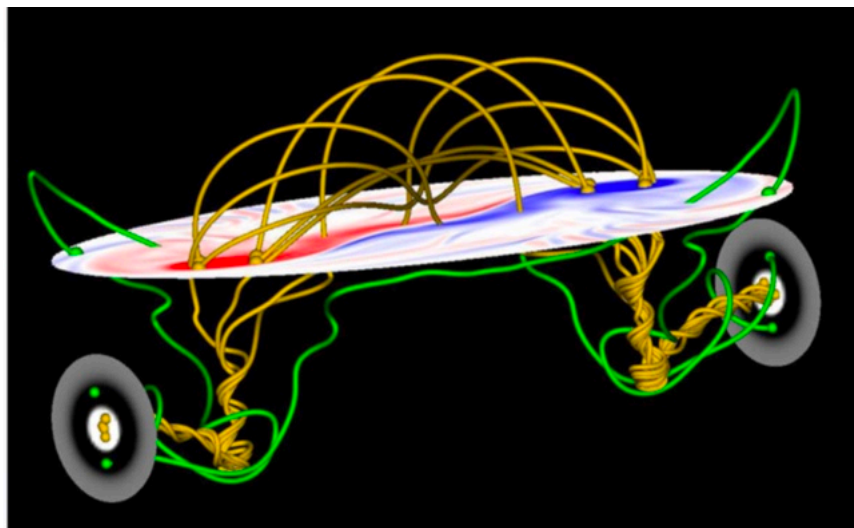


# Non-neutralized AR Currents as Proxy for Eruptive Activity



Yang Liu (HEPL/SU)

Tibor Török (PSI)

Slava Titov (PSI)

James Leake (GSFC)

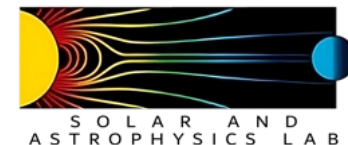
Xudong Sun (IfA/UH)

Meng Jin (LMSAL)

Stanford University



Predictive Science, Inc.



Work supported by NASA, NSF, and NRL. Publication: Liu *et al.*, ApJ **961**, 148 (2024)

# Abstract

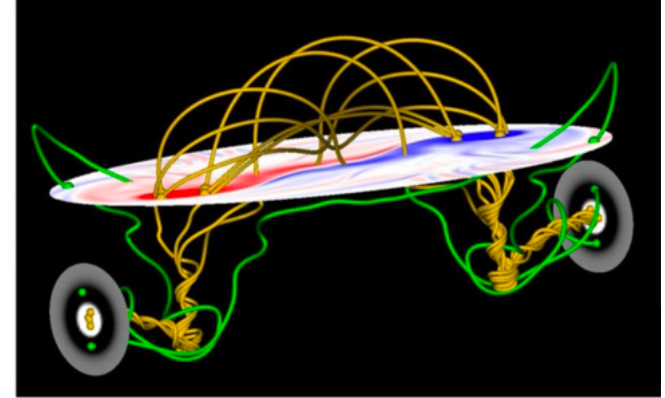
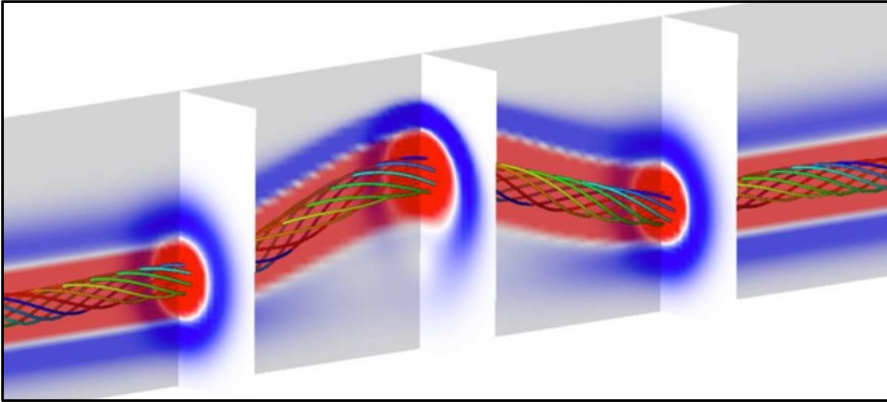
Many proxies for assessing the eruptive activity of solar active regions (ARs) have been suggested, mostly based on measurements of the photospheric magnetic field.

Here we test the usefulness of  $|DC/RC|$  (ratio of photospheric direct to return current) for assessing the ability of ARs to produce CMEs, and compare it with the amount of shear along the eruptive section of the polarity inversion line (PIL).

We find that all source regions of eruptive flares have  $|DC/RC| > 1.63$  and PIL shear  $> 45^\circ$  (3.2 and  $68^\circ$  on average), tending to be larger for stronger events. Both quantities are on average smaller for source regions of confined flares (2.2 and  $46^\circ$ ), albeit with substantial overlap. Many source regions, especially those of eruptive X-class flares, exhibit elongated direct currents (EDCs) bracketing the eruptive PIL segment, typically coinciding with areas of continuous PIL shear  $> 45^\circ$ . However, a small subset of confined flares have  $|DC/RC|$  close to unity, very low PIL shear ( $< 38^\circ$ ), and no clear EDC signatures, rendering such regions less likely to produce a CME.

A simple quantitative analysis reveals that  $|DC/RC|$  and PIL shear are almost equally good proxies for assessing CME-productivity, and comparable to other proxies suggested in the literature. We also demonstrate that an inadequate selection of the current-integration area typically yields a substantial underestimation of  $|DC/RC|$ .

# Introduction I

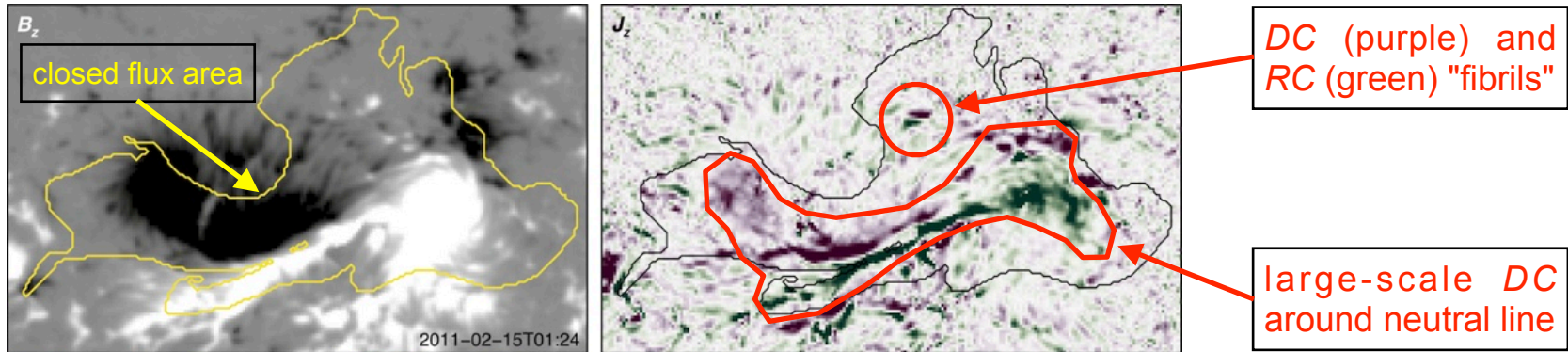


MHD simulation of flux emergence. *Left*: current-neutralized sub-photospheric flux rope (red/blue: direct/return current). *Right*: After emergence into the corona, the flux rope carries mainly direct current (Török *et al.* 2014).

In an isolated magnetic flux rope (as thought to exist in the convection zone), electric currents are *neutralized*: the central **direct current (DC)** is surrounded by an oppositely directed **return current (RC)** of same strength ( $|DC/RC| = 1$ ; top left image). On the other hand, magnetically non-isolated flux ropes (as in the corona), can carry a substantial **net current** ( $|DC/RC| > 1$ ; top right image).

In well-isolated ARs, the currents are *balanced*, i.e., all currents that flow into an AR ( $j_z > 0$ ) flow also out of it ( $j_z < 0$ ). However, there has been a long-lasting debate on whether or not AR-currents are additionally neutralized (Parker 1996; Melrose 1996), which requires the sum of all in- and out-flowing currents to be zero also within each AR polarity. Recent simulations (e.g., Török & Kliem 2003; Török *et al.* 2014; Dalmasse *et al.* 2015) suggest that current-neutralization breaks down if significant shear develops along the PIL, as typically seen in eruptive ARs.

# Introduction II



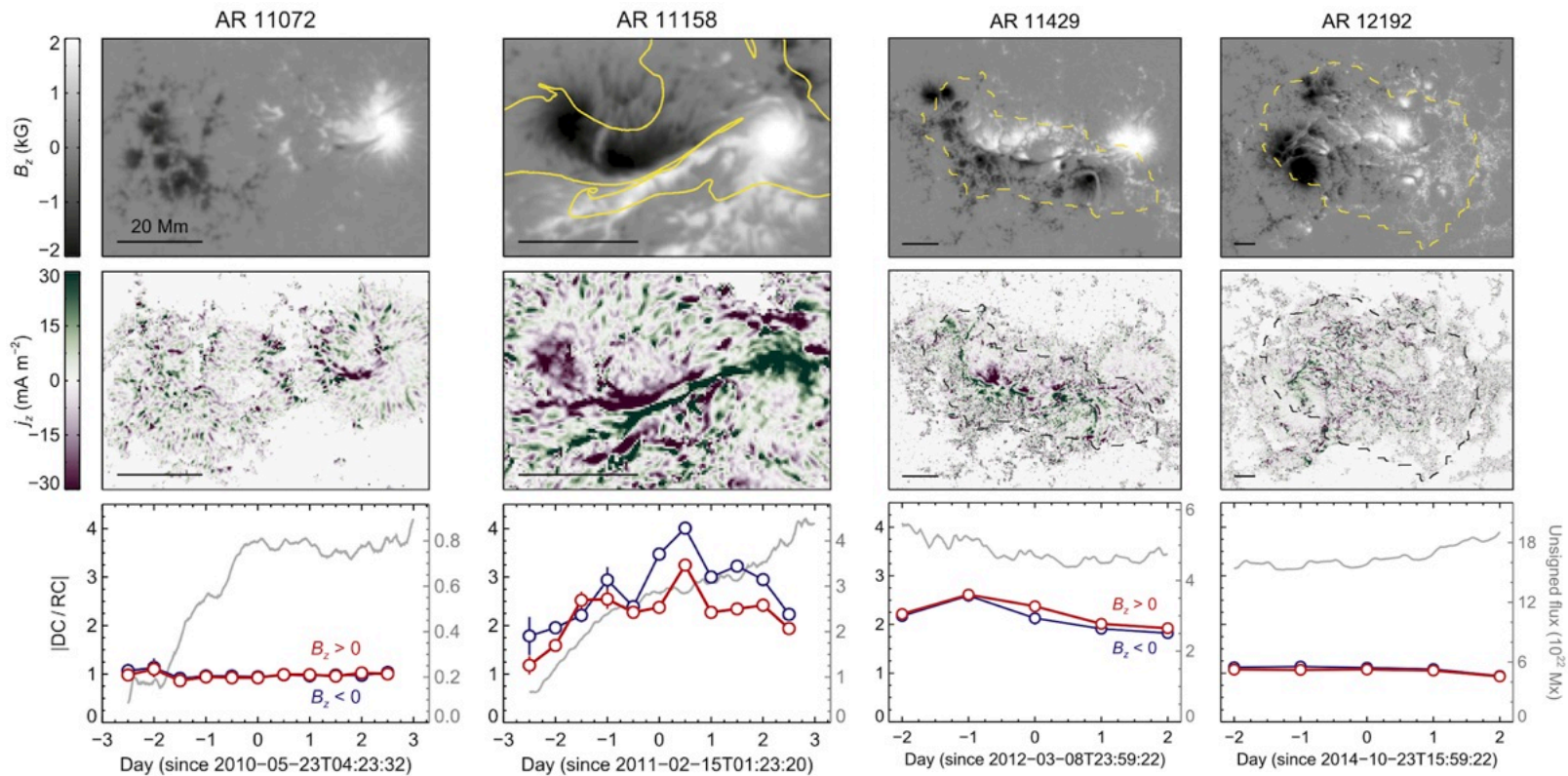
HMI observations of AR 11158 (left:  $B_z$ ; right:  $J_z$ ). From [Liu et al. \(2017\)](#).

HMI observations indicate that ARs (unlike single flux ropes) contain many "fibril-like" direct and return currents that seem to cancel out, so that the whole AR is neutralized (as suggested by [Parker 1996](#)). However, some ARs additionally show a strong direct current surrounding the PIL (e.g., [Georgoulis et al. 2012](#)), indicative of the presence of a non-neutralized flux rope (or strongly sheared magnetic arcade) in the AR center (supporting the suggestion by [Melrose 1996](#)).

**Our hypothesis:** Since strong net currents indicate the presence of flux ropes, they may serve as a proxy for the capability of an AR to produce a CME.

**Our approach:** Measure  $|DC/RC|$  for AR sample and relate to eruptive activity. Evaluate  $|DC/RC|$  only in closed-flux area above eruptive PIL (estimated using squashing factor and flare observations), as adjacent flux is irrelevant.

# Pilot study with (only) four cases (Liu *et al.*, 2017)



| AR       | $\langle  DC/RC  \rangle$ | $\langle \Phi \rangle$      | <i>J</i> -pattern | Flares | CMEs |
|----------|---------------------------|-----------------------------|-------------------|--------|------|
| AR 11072 | $0.98 \pm 0.01$           | $25^\circ 1 \pm 6^\circ 4$  | No                | No     | No   |
| AR 12192 | $1.06 \pm 0.01$           | $41^\circ 2 \pm 11^\circ 3$ | No                | Yes    | No   |
| AR 11429 | $2.17 \pm 0.01$           | $67^\circ 4 \pm 8^\circ 5$  | Yes               | Yes    | Yes  |
| AR 11158 | $2.54 \pm 0.02$           | $63^\circ 6 \pm 6^\circ 9$  | Yes               | Yes    | Yes  |

5-day average values;  $\langle \Phi \rangle$ : average shear angle along PIL; *J*-pattern: elongated current around PIL

(Preliminary) conclusion:  $|DC/RC|$  is a better proxy for assessing the ability of an AR to produce CMEs

# Larger Sample

Ratio of the Total Direct to Total Return Current,  $|DC/RC|$ , and Magnetic Shear along the PIL for Strong Flares (X and M Class) with and without CMEs and for Weak Flares with CMEs (See Text for Details)

| AR                 | Date and Time     | Flare/<br>CME | Position | $ DC/RC ^{+}$<br>$B_z > 0$ | $ DC/RC ^{-}$<br>$B_z < 0$ | $ DC/RC $<br>mean | Shear<br>(deg) | EDC |
|--------------------|-------------------|---------------|----------|----------------------------|----------------------------|-------------------|----------------|-----|
| <b>Group 1</b>     |                   |               |          |                            |                            |                   |                |     |
| 11158*             | 2011.02.15, 01:44 | X2.2 Y        | S21W10   | $2.841 \pm 0.060$          | $3.378 \pm 0.094$          | $3.110 \pm 0.380$ | $75.9 \pm 1.7$ | Y   |
| 11283              | 2011.09.06, 22:12 | X2.1 Y        | N14W18   | $3.602 \pm 0.142$          | $4.650 \pm 0.255$          | $4.126 \pm 0.741$ | $73.4 \pm 0.2$ | Y   |
| 11429*             | 2012.03.07, 00:02 | X5.4 Y        | N17E24   | $2.567 \pm 0.048$          | $2.560 \pm 0.038$          | $2.564 \pm 0.031$ | $74.0 \pm 0.1$ | Y   |
| 11515              | 2012.07.06, 23:01 | X1.1 Y        | S17W50   | $4.670 \pm 0.199$          | $4.722 \pm 0.270$          | $4.696 \pm 0.168$ | $81.3 \pm 0.7$ | Y   |
| 11520              | 2012.07.12, 15:37 | X1.4 Y        | S17W08   | $2.770 \pm 0.070$          | $2.652 \pm 0.058$          | $2.711 \pm 0.083$ | $60.8 \pm 0.1$ | ?   |
| 11890              | 2013.11.05, 22:07 | X3.3 Y        | S09E36   | $6.267 \pm 0.339$          | $7.716 \pm 0.337$          | $6.992 \pm 1.024$ | $73.1 \pm 0.5$ | Y   |
| 12017              | 2014.03.29, 17:35 | X1.0 Y        | N10W32   | $2.299 \pm 0.069$          | $2.308 \pm 0.070$          | $2.304 \pm 0.049$ | $60.5 \pm 0.3$ | Y   |
| 12158              | 2014.09.10, 17:21 | X1.6 Y        | N15E02   | $2.114 \pm 0.052$          | $2.519 \pm 0.070$          | $2.317 \pm 0.286$ | $63.1 \pm 0.4$ | ?   |
| 12205              | 2014.11.07, 16:53 | X1.6 Y        | N15E33   | $3.498 \pm 0.091$          | $2.617 \pm 0.057$          | $3.058 \pm 0.623$ | $74.7 \pm 0.4$ | Y   |
| 12242 <sup>+</sup> | 2014.12.20, 00:11 | X1.8 Y        | S18W29   | $2.165 \pm 0.039$          | $2.390 \pm 0.052$          | $2.278 \pm 0.159$ | $67.9 \pm 0.3$ | Y   |
| 12297              | 2015.03.11, 16:11 | X2.1 Y        | S16E13   | $5.120 \pm 0.193$          | $2.360 \pm 0.058$          | $3.740 \pm 1.952$ | $68.8 \pm 1.3$ | Y   |
| 12673              | 2017.09.06, 11:53 | X9.3 Y        | S09W38   | $6.683 \pm 0.149$          | $4.530 \pm 0.095$          | $5.607 \pm 1.522$ | $73.8 \pm 6.0$ | Y   |
| <b>Group 2</b>     |                   |               |          |                            |                            |                   |                |     |
| 11166 <sup>+</sup> | 2011.03.07, 13:45 | M1.9 Y        | N11E13   | $1.885 \pm 0.121$          | $1.547 \pm 0.043$          | $1.716 \pm 0.239$ | $51.2 \pm 3.8$ | N   |
| 11261              | 2011.08.02, 05:19 | M1.4 Y        | N16W08   | $3.781 \pm 0.144$          | $3.194 \pm 0.113$          | $3.488 \pm 0.415$ | $70.0 \pm 0.1$ | Y   |
| 11305              | 2011.10.02, 00:37 | M3.9 Y        | N11W12   | $3.135 \pm 0.123$          | $3.113 \pm 0.124$          | $3.124 \pm 0.087$ | $70.1 \pm 0.2$ | ?   |
| 11667              | 2013.02.06, 00:04 | C8.7 Y        | N22E14   | $1.767 \pm 0.098$          | $1.513 \pm 0.095$          | $1.640 \pm 0.180$ | ...            | N   |
| 11817              | 2013.08.12, 10:21 | M1.5 Y        | S22E14   | $2.992 \pm 0.104$          | $2.654 \pm 0.081$          | $2.823 \pm 0.239$ | $46.1 \pm 2.8$ | Y   |
| 12027              | 2014.04.04, 13:34 | C8.3 Y        | N13E23   | $1.978 \pm 0.218$          | $1.527 \pm 0.094$          | $1.753 \pm 0.319$ | ...            | N   |
| <b>Group 3</b>     |                   |               |          |                            |                            |                   |                |     |
| 11166 <sup>+</sup> | 2011.03.09, 23:13 | X1.5 N        | N11W15   | $1.026 \pm 0.020$          | $1.153 \pm 0.017$          | $1.090 \pm 0.090$ | $37.1 \pm 2.6$ | ?   |
| 11476              | 2012.05.10, 04:11 | M5.7 N        | N13E22   | $4.152 \pm 0.174$          | $6.665 \pm 0.324$          | $5.408 \pm 1.777$ | $63.1 \pm 1.2$ | Y   |
| 11520              | 2012.07.10, 04:58 | M1.7 N        | S17E27   | $2.294 \pm 0.062$          | $2.836 \pm 0.065$          | $2.565 \pm 0.383$ | $49.9 \pm 2.9$ | Y   |
| 11875              | 2013.10.24, 09:59 | M2.5 N        | N06W14   | $1.893 \pm 0.048$          | $1.727 \pm 0.047$          | $1.810 \pm 0.117$ | $48.2 \pm 3.9$ | ?   |
| 11967              | 2014.02.04, 03:57 | M5.2 N        | S16W06   | $3.019 \pm 0.045$          | $2.256 \pm 0.045$          | $2.638 \pm 0.540$ | $46.9 \pm 1.7$ | Y   |
| 12192*             | 2014.10.24, 21:07 | X3.1 N        | S14E15   | $1.036 \pm 0.011$          | $1.005 \pm 0.010$          | $1.021 \pm 0.022$ | $26.5 \pm 1.4$ | N   |
| 12222              | 2014.12.04, 18:05 | M6.1 N        | S20W32   | $1.085 \pm 0.022$          | $1.044 \pm 0.024$          | $1.065 \pm 0.029$ | $26.1 \pm 6.2$ | ?   |
| 12242 <sup>+</sup> | 2014.12.19, 09:31 | M1.3 N        | S18W23   | $1.148 \pm 0.029$          | $1.162 \pm 0.028$          | $1.155 \pm 0.020$ | $32.5 \pm 0.5$ | N   |
| 12268              | 2015.01.29, 11:32 | M2.1 N        | S12W06   | $2.861 \pm 0.155$          | $2.947 \pm 0.205$          | $2.904 \pm 0.104$ | $75.7 \pm 0.4$ | ?   |
| 12422              | 2015.09.28, 14:53 | M7.6 N        | S20W16   | $1.978 \pm 0.041$          | $2.182 \pm 0.061$          | $2.080 \pm 0.144$ | $57.5 \pm 3.8$ | Y   |

Group 1:  
12 eruptive  
X flares

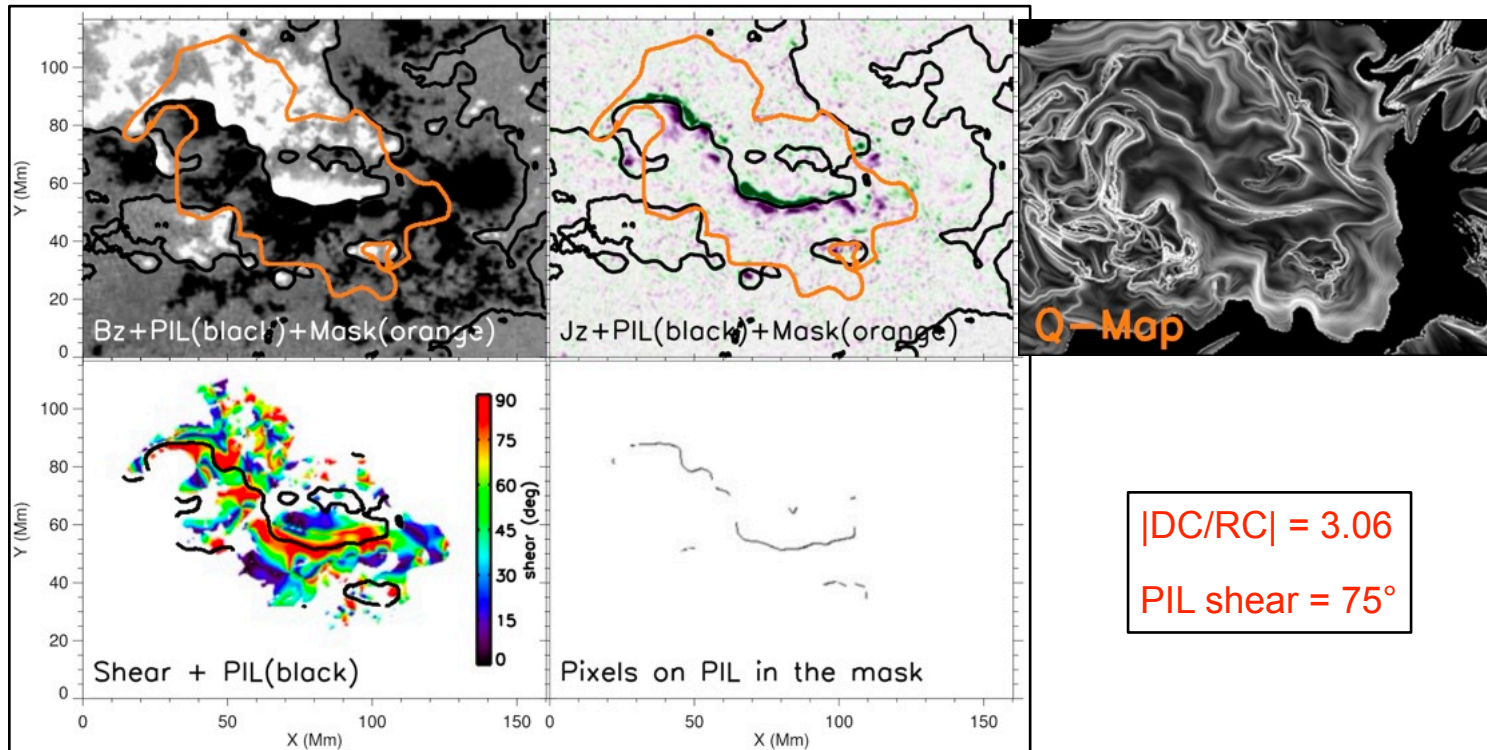
Group 2:  
6 eruptive  
C/M flares

Group 3:  
10 confined  
M/X flares

**Note.** ARs that produced events in *different* source regions (PIL segments) are marked with a plus sign; ARs that were investigated also in Liu et al. (2017) are marked with an asterisk. EDC stands for “Elongated Direct Current,” i.e., the presence of a (often double-*J*-shaped) pattern of an elongated, coherent direct-current concentration bracketing the PIL (“Y,” “N,” and “?” stand for yes, no, and ambiguous, respectively).

$|DC/RC|$  and (average) PIL shear are *single* values; taken shortly before respective eruption

# One Example



AR 12205 shortly before eruptive X1.6 flare on November 7, 2014

$$|DC/RC| = 3.06$$

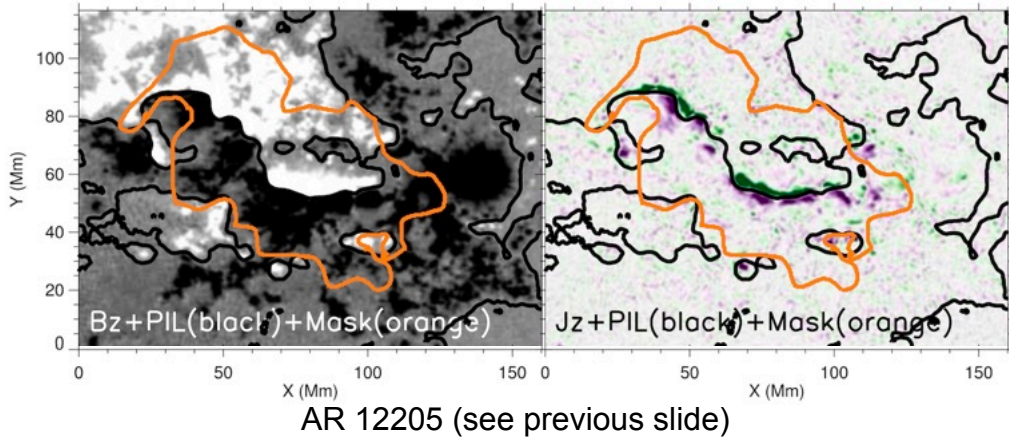
$$\text{PIL shear} = 75^\circ$$

(1) Integration area (“mask”; orange contour) = closed flux above eruptive PIL segment; guided by flare extension and squashing-factor Q-maps obtained from NLFFF extrapolation (top right).

(2) Integrate  $J_z > 0$  and  $J_z < 0$  within mask for each polarity separately, using only pixels with  $B > 300$  G  $\rightarrow |DC/RC|^+$ ,  $|DC/RC|^- \rightarrow |DC/RC| = (|DC/RC|^+ + |DC/RC|^-) / 2$ .

(3) Average shear along PIL pixels within mask, again only for  $B > 300$  G (bottom right)

# $|DC/RC|$ Dependence on Integration Area



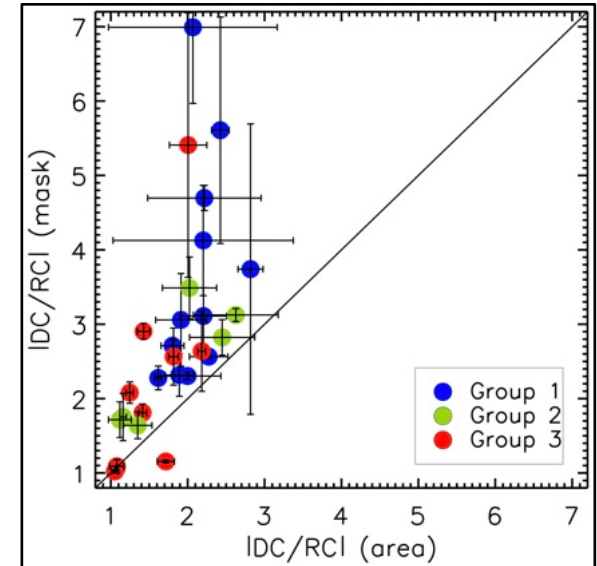
$|DC/RC|^{+} = 3.50$  (2.15 for whole area shown)

$|DC/RC|^{-} = 2.62$  (1.68 for whole area shown)

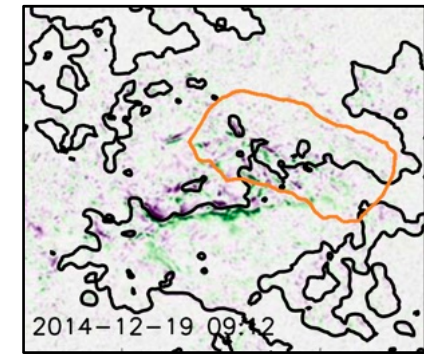
(presumably even smaller if whole AR were chosen)

$|DC/RC|$  can depend strongly on the chosen integration area, especially for complex ARs where current systems not involved in a specific eruption may be present (see example to the right).

$|DC/RC|$  is typically underestimated if the integration area is chosen too large, and likely overestimated if it is chosen too narrow (i.e., only close to the PIL; see [Kazachenko et al., 2022](#))

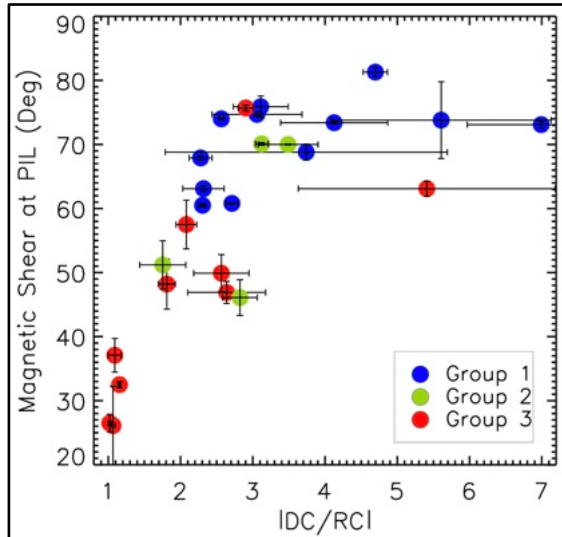


$|DC/RC|$  obtained by “mask” vs. “area” methods, shown for complete sample



$J_z$  in AR 12242 prior to confined flare. Strong currents exist outside eruptive area (orange)

# Main Results

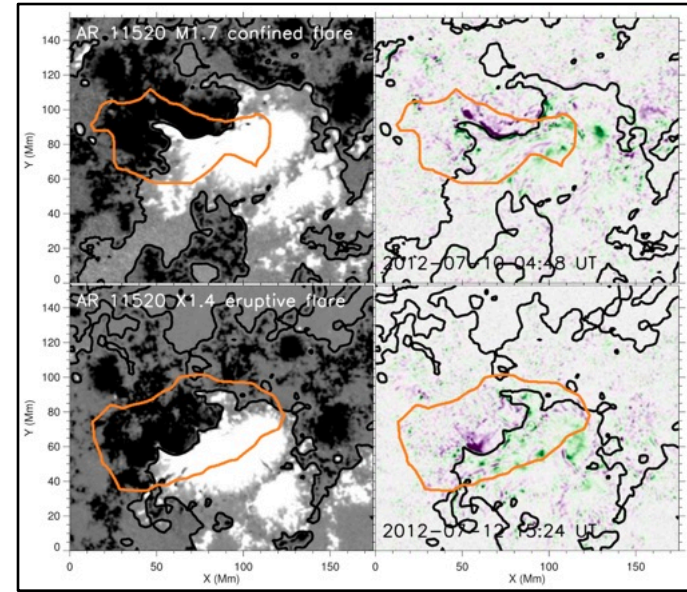


$|DC/RC|$  vs. PIL shear (using “mask” method)

**Group 1:**  $|DC/RC|$  2.3-7.0 ( $\langle 3.6 \rangle$ ); PIL shear  $61^\circ$ - $81^\circ$  ( $\langle 71^\circ \rangle$ )

**Group 2:**  $|DC/RC|$  1.6-3.5 ( $\langle 2.4 \rangle$ ); PIL shear  $46^\circ$ - $70^\circ$  ( $\langle 59^\circ \rangle$ )

**Group 3:**  $|DC/RC|$  1.0-5.4 ( $\langle 2.2 \rangle$ ); PIL shear  $26^\circ$ - $76^\circ$  ( $\langle 46^\circ \rangle$ )



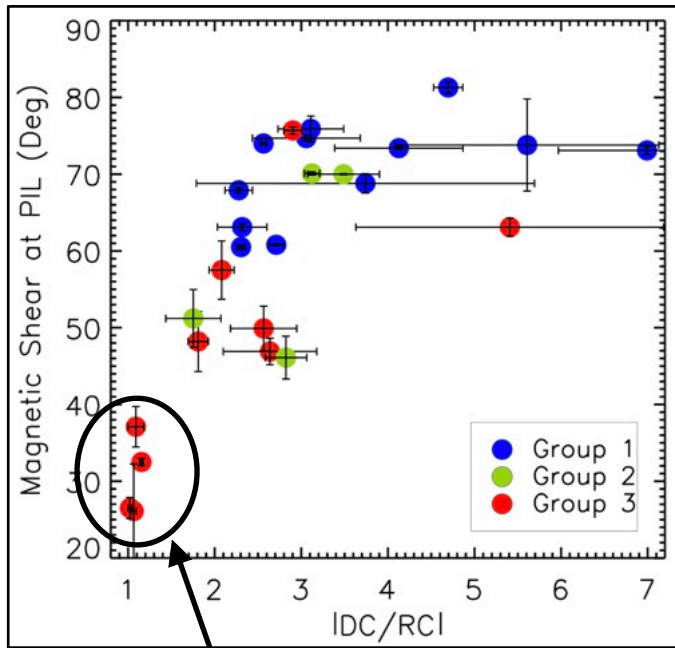
Confined and eruptive flare from the same PIL (2.5 days apart).  $|DC/RC|=2.57$  (2.71) and PIL shear =  $50^\circ$  ( $61^\circ$ ) for the confined (eruptive) flare.

All CME-producing source regions have  $|DC/RC| > 1.63$  and shear  $> 45^\circ$ , tending to be larger for stronger events. The values are smaller for confined events, albeit with substantial overlap, as source regions with large values can sometimes produced both eruptive and confined flares (see top right).

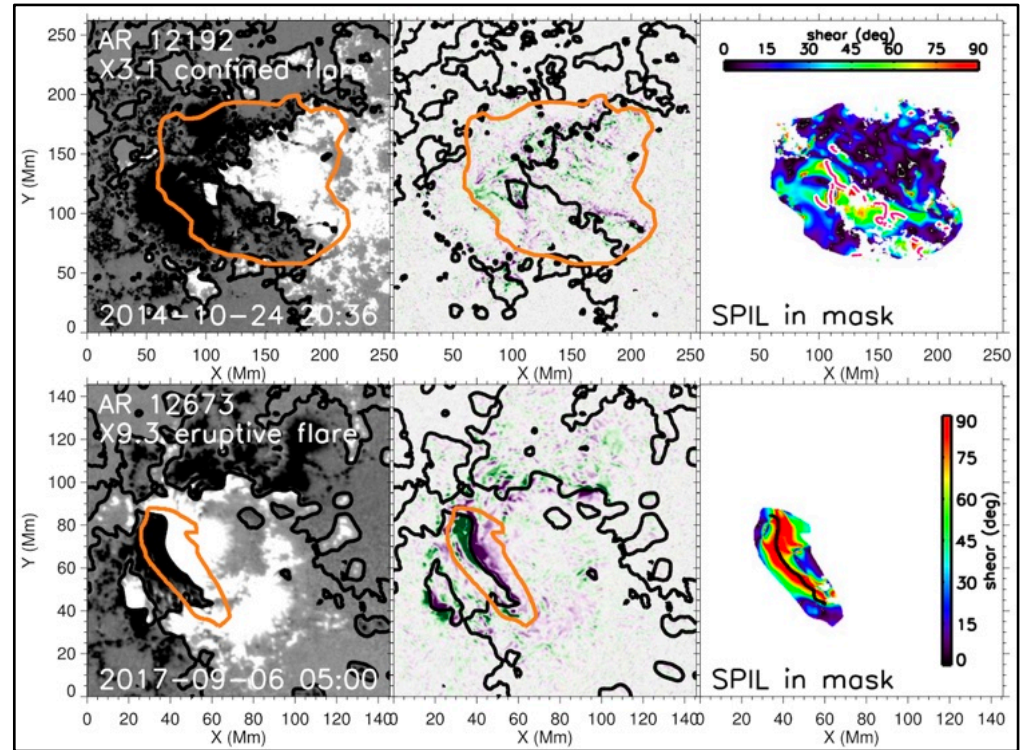
Many source regions (especially of eruptive X-flares) have elongated direct currents (EDCs) coinciding with continuous PIL shear  $> 45^\circ$  (SPIL), indicative of a flux rope or sheared magnetic arcade.

Using thresholds  $|DC/RC|=2.2$  & PIL shear  $60^\circ$  (Group 1 minima), both quantities predict CME occurrence with similar probability (80-90%), comparable to other proxies (e.g., [Li+ 2022](#); [Falconer+ 2008](#)).

# Special Subset of Confined Flares



$|DC/RC|$  vs. PIL shear (using “mask” method)



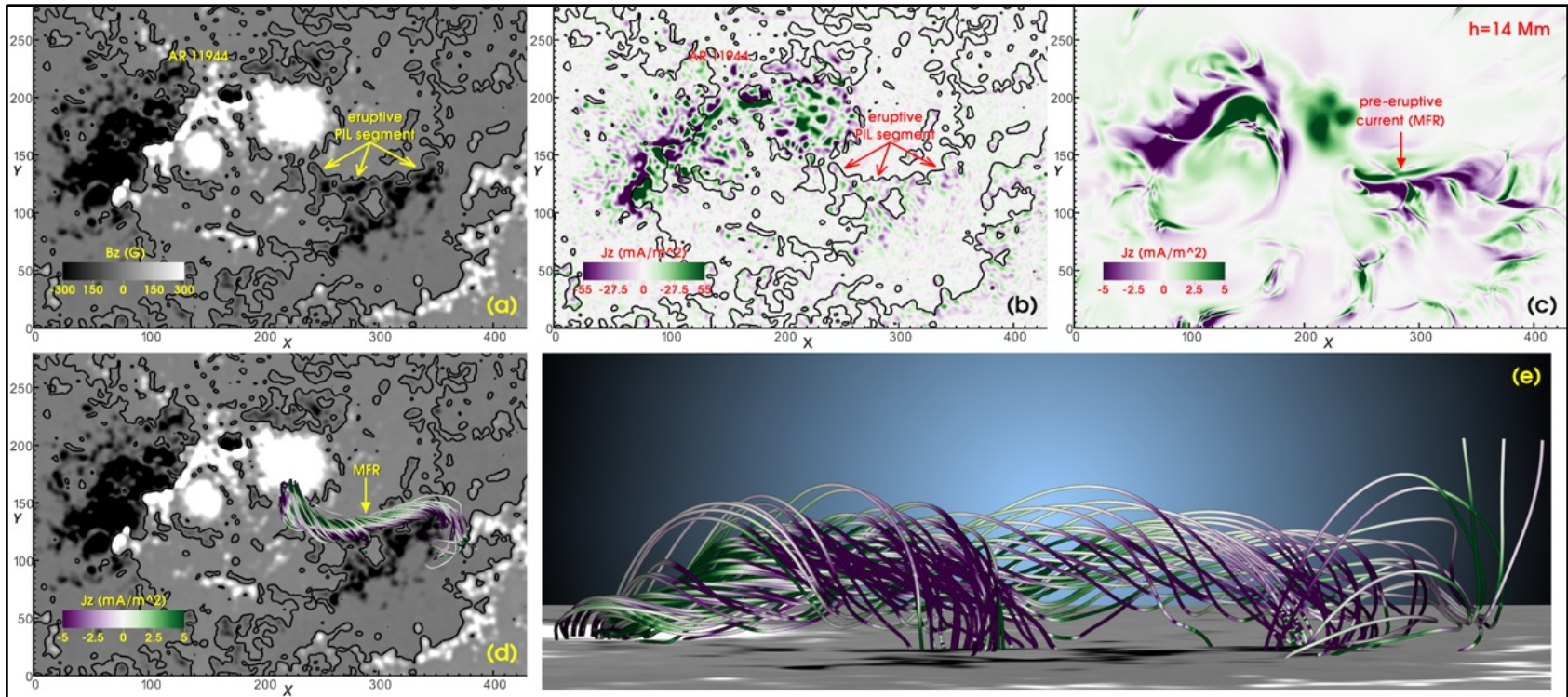
Top:  $|DC/RC|=1.02$ , PIL shear  $27^\circ$ , no EDC, no coherent SPIL

Bottom:  $|DC/RC|=5.61$ , PIL shear  $74^\circ$ , EDC & coherent SPIL

(Small) subgroup of confined flares characterized by (1)  $|DC/RC|$  close to unity, (2) very low PIL shear ( $< 38^\circ$ ), and (3) absence of an EDC or coherent SPIL (see AR 12192 on the top right)

This suggests that such source regions are unlikely to produce CMEs. However, see the “counterexample” on the next slide. Follow-up studies with larger samples are needed.

# A "Counterexample:" the January 7, 2014 eruption



No indications of strong fields, organized currents (EDC), or a SPIL along eruptive PIL segment ( $B < 300$  G, so we did not include this event in our sample)

Yet, the eruption produced a strong X1.2 flare and a very fast CME ( $\approx 2400$  km/s)

NLFFF extrapolation suggests that the current channel (EDC) was located largely in the low corona (with one foot compactly rooted in the sunspot and the other spread out over dispersed polarities)

# Conclusions

(1) Contrary to Liu et al. 2017, we find that  $|DC/RC|$  and PIL shear are equally good proxies for assessing the ability of an AR to produce CMEs, and comparable to other proxies that have been suggested (e.g., twist / flux)

(2) The predictive quality of such proxies is likely to improve if coronal quantities (e.g., decay index of the ambient coronal magnetic field) are incorporated.

(3) Our results indicate that a specific type of source regions can produce strong flares but no CMEs. However, larger samples are needed to test this conjecture.

(4) Future studies should, therefore, also distinguish between “Type I” (eruption) and “Type II” (only reconnection) confined eruptions ([Li et al. 2019](#)).

# References

- Avallone & Sun 2020, ApJ **893**, 123
- Dalmasse *et al.* 2015, ApJ **810**, 17
- Falconer *et al.* 2008, ApJ **689**, 1433
- Georgoulis *et al.* 2012, ApJ **761**, 61
- Kazachenko *et al.*, ApJ **926**, 56
- Li *et al.* 2019, ApJ **881**, 151
- Li *et al.* 2022, ApJL **926**, L14
- Liu *et al.* 2017, ApJL **846**, L6
- Melrose 1996, ApJL **471**, 497
- Parker 1996, ApJL **471**, 489
- Török *et al.* 2014, ApJL **782**, L10
- Török & Kliem 2003, A&A **406**, 1043